Breathing behavior of coupled Bose-Einstein condensates: from multi-soliton interactions to homoclinic tangles

R. Carretero-González*,[1] and K. Promislow[2]

[1] *Nonlinear Dynamical Systems Group†, Computational Science Research Center, and Department of Mathematics & Statistics, San Diego State University, San Diego, CA 92182-7720, USA.*
[2] *Department of Mathematics, Michigan State University, East Lansing, MI 48824, USA.*

(Dated: To be submitted to *PRE*, September 25, 2008)

We consider the interaction of Bose-Einstein condensates in a nonlinear lattice formed from the local minima of an externally imposed periodic potential. Within a one-dimensional geometry, we develop a perturbation expansion for the motion of a condensate within the confines of the local minima of its potential well, coupled to the near-neighbor interaction with the adjacent condensates. We show that the resultant system of lattice differential equations possesses spatially localized breathing solutions.

I. INTRODUCTION

More than three quarters of a century ago, Bose and Einstein predicted that a gas at very low temperatures and densities turns into a Bose-Einstein condensate that can be described by what is called now Bose-Einstein statistics [1, 2]. In a Bose-Einstein condensate (BEC), all the atoms share the same quantum state. This novel state of matter, which exists at temperatures only a few billionths of a degree above absolute zero, was first achieved experimentally in the mid-1990's, see Refs. [3, 4]. Recent advances in cooling techniques have triggered a vast experimental and theoretical investigation of the novel dynamics of BECs [5].

A mean field approach, which neglects three body collisions, allows for the macroscopic description of the BEC through the Gross-Pitaevskii (GP) equation [5–7]

$$\mathrm{i}\hbar\frac{\partial\varphi}{\partial t}=\left(-\frac{\hbar^2\nabla^2}{2m}+V_{\mathrm{ext}}(\vec{r})+g_0|\varphi|^2\right)\varphi, \qquad (1)$$

where $\varphi=\varphi(\vec{r},t)$ is the condensate wave function and $|\varphi(\vec{r},t)|^2$ physically represents the density distribution of atoms in the condensate. The inter-atomic interactions are described by an effective coupling constant [5, 8]

$$g_0=\frac{4\pi\hbar^2 a}{m}$$

where a is the scattering length and m the atomic mass of the atoms inside the BEC. The scattering length a is negative (positive) for attractive (repulsive) atomic species [5]. In this work we deal with attractive species ($a<0$) that support bright soliton structures in the one-dimensional setup [5]. The total external potential $V_{\mathrm{ext}}(\vec{r})$ is comprised of a confining magnetic potential V_{conf} in which the BEC is grown and a manipulating potential, V_{per}, which is typically periodic with a period much smaller than the spatial scale of the confining potential,

$$V_{\mathrm{ext}}(\vec{r})=V_{\mathrm{conf}}(\vec{r})+V_{\mathrm{per}}(\vec{r}).$$

Of particular interest is the dynamics of BECs which are localized within a periodic potential generated by counter propagating laser beams [9–14]. The superposition of a number of interference patterns with the appropriate spatial periodicity permits the construction of a wide variety of periodic potentials. Indeed, novel techniques for manipulating the condensates, including micro-magnetic guides [15] and the growth of condensate on a grated surface, chips or lithograpically imprinted surface [16–19], open up a host of possible applications.

In this paper we consider a cigar-shaped condensate with two strongly confined transverse directions (arising from the confining magnetic potential) for which the dynamics along the principle axis of the cigar-shape can be accurately described by the *one*-dimensional GP equation [5, 8, 20–22, 24–26]:

$$\mathrm{i}u_t+\frac{1}{2}u_{xx}+|u|^2u=V(x)u, \qquad (2)$$

where $u=u(x,t)$, the subscripts denote partial derivatives, and the physical quantities (time, space, BEC density, potential) have been nondimensionalized [5, 22]. As a further simplification the confining potential is neglected and the potential is taken to be completely periodic. The actual form of the local minima is not essential to the analysis, the square of the Jacobi elliptic sine function

$$V(x)=V_0\,\mathrm{sn}^2(x;k), \qquad (3)$$

is taken since the local wells are well approximated by tanh functions as $k\to 1$, where k is the elliptic modulus.

The main aim of the present work is to find localized oscillations (breathers) [23] supported in chains of couple bright solitons (slightly pinned to their respective minima of the periodic potential) and some of their properties. Specifically, the manuscript is organized as follow. In Sec. II we describe the the oscillations of single (uncoupled) bright solitons inside the potential minima of the

*URL: http://www.rohan.sdsu.edu/∼rcarrete
†URL: http://nlds.sdsu.edu/

perioc external potential using a conservation approach and its improvement via pertubation theory. We also briefly study the weak radiation loss of this oscillatory process. In Sec. III we analyzed the soliton-soliton interactions wtihout the presence of the external pontential and obtain a reduced differential equation on the soliton's position described by a real Toda lattice. Sec. IV is devoted to validate the lattice differential equation that is obtained by combining the soliton-potential and soliton-soliton interactions. In Sec. V we construct localized oscillations supported by the soliton chain and analyze some of its properties such as robustness, mobility and collisions. Finally, in Sec. VI we conclude with a brief overview of our approach and the possible extensions and applications.

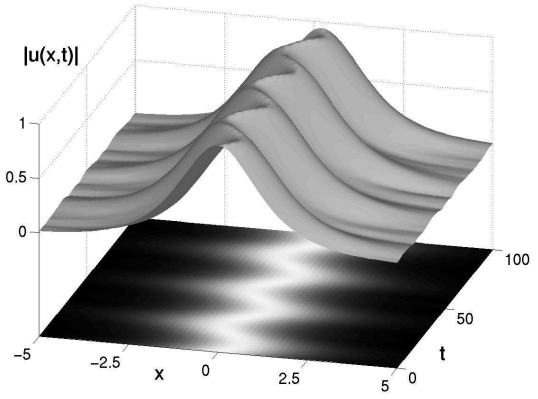

FIG. 1: A single conglomerate of condensate oscillating inside the potential $V(x)$ (4). The potential strength is $V_0 = 0.1$ and the initial velocity of the soliton is $v_0 = 0.1$.

II. SOLITON OSCILLATIONS

The first step to decribe the coupled dynamics of the soliton train inside the periodic potential is to describe the interaction of a single soliton with the respective local minimum of the potential. For small perturbations, each (uncoupled) soliton performs oscillations about their respective local potential minimum (see Fig. 1). We characterise below this behavior with two different approaches: a) using the conservation of mass and energy (Sec. II A) and b) employing a perturbation approach (Sec. II B).

A. Conservation approach

In order to find approximate equations for the oscillatory movement we use an appropriate ansatz approach together with the mass and energy conservation as in Ref. [27]. The GP equation (2) with $V_0 = 0$ is completely integrable and posseses an infinite number of conserved quantities. Nevertheless, for $V_0 \neq 0$, it still admits the total mass N (number of atoms in the condensate) and energy E [see Eqs. (A1)] to be conserved under the evolution of Eq. (2).

Let us consider the case of a single soliton inside a single potential through. This corresponds to the limit $k \to \infty$ that yields a potential

$$V(x) = V_0 \tanh^2(x), \tag{4}$$

whose steady state solution (i.e., when the soliton is centered at the bottom of the potenital) is given by [28]

$$u_0(x,t) = H \,\mathrm{sech}(x) e^{-\mathrm{i}(1/2 - V_0)t}. \tag{5}$$

Let us now allow for the amplitude $H(t)$, width $\nu(t)$ and position $\xi(t)$ of the soliton to be time dependent parameters:

$$u(x,t) = H(t)\,\mathrm{sech}\left(2\nu(x-\xi(t))\right) e^{-\mathrm{i}(1/2 - V_0)t}. \tag{6}$$

Then, using the conservation of mass and energy ($dN/dt = 0 = dE/dt$) and approximating the overlapping integral between the soliton and the potential (see Appendix A for details) yields the follwoing Newtonian equation of motion for the center of the solitons:

$$\ddot{\xi} = -V'_{\mathrm{eff1}}(\xi) \tag{7}$$

with an effective potential

$$V_{\mathrm{eff1}}(\xi) \approx 2\nu V_0 \left[\frac{4}{15}\xi^2 - \frac{4}{63}\xi^4\right], \tag{8}$$

where the width $\nu = 1/2$ corresponds to a resting soliton.

We now compare the oscillation frequency from the effective potential (8) against the numerically computed results obtained from directly integrating the GP equation (2). Imposing a relation between initial pulse velocity, v_0, and well amplitude, V_0, assures that the dynamics belong in the appropriate small-amplitude regime. Figure 2 shows the behavior for the oscillation frequency for an initial soliton velocity of $v_0 = V_0/5$. The frequency of oscillation obtained by the energy approach (green dashed line) does not coincide exactly with the numerical results (red circles), except in the case when $V_0 \to 0$ (see inset in the figure).

B. Perturbative analysis

In order to improve upon the above conservative approach we now employ a perturbative analysis to more accurately describe the oscillatory behavior of a single hump of Bose-Einstein condensate inside a single well of the form (4). We rewrite the exact stationary (static soliton centered at the minima of the well) solution (5) as

$$u_0(x,t) = R_0(x)\, e^{-\mathrm{i}\omega_0 t}, \tag{9}$$

where

$$R_0(x) = \sqrt{1 - V_0}\; S(x), \tag{10}$$

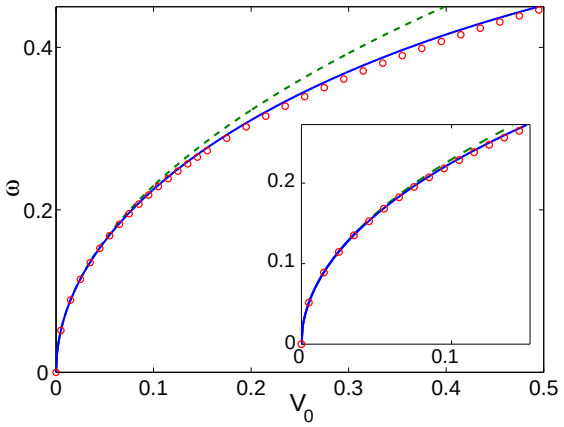

FIG. 2: (Color online). Frequency of the oscillating soliton ω as a function of potential strength V_0. The numerical experiments for $V_0 = 0.1$ and $v_0 = V_0/5$ for the full NLS simulation are depicted with circles. The frequency obtained using V_{eff1} (8) by the energy approach is depicted with the green dashed line, while the blue solid line corresponds to V_{eff2} (13) obtained from the perturbative approach.

with $S(x) = \text{sech}(x)$ and $\omega_0 = \frac{1}{2} - V_0$. To describe the deformation of the soliton solution as it oscillates, and more accurately capture the true period of the oscillation we consider a general perturbation to the stationary state (9) of the form

$$u(x,t) = R(x-\xi)\, e^{\mathrm{i}\rho(x-\xi,t)}, \tag{11}$$

where

$$\begin{aligned} R(s) &= R_0(s) + V_0\, \psi(s, V_0) \\ \rho(s,t) &= v\, s + \omega\, t. \end{aligned} \tag{12}$$

Here ψ (the shape correction) is a real function, v and ξ, respectively the velocity and position, are time dependent scalars, and ω is the frequency.

After expanding phase, position and shape correction on the small parameter V_0, solving to second order in V_0 and keeping terms up to third order in ξ (see Appendix B for details) yields the following form for the effective potential

$$V_{\text{eff2}}(\xi) \approx V_0 \left[\left(\frac{4}{15} - \frac{112}{1125} V_0 \right) \xi^2 - \frac{4}{63} \xi^4 \right]. \tag{13}$$

This new effective potential (13) gives a much better approximation to the oscillation frequency (cf. blue solid curve in Fig. 2) over a large span of potential amplitudes V_0 (relative error of less than 2% over the range of velocities considered).

C. Radiation of a single BEC hump

We show via numerical simulation that radiation loss is indeed present but that the rate of dissipation is very small (compared to typical oscillation times). The radiation loss damps the oscillation amplitude for the soliton parameters. The radiated energy is absorbed by the boundary conditions. These damping boundary conditions are achieved by multiplying the solution by $1+\delta(x)$ at every time step, where $\delta(x)$ is a smooth function such that $\delta \ll 1$ near the boundaries and $\delta = 0$ inside the domain. Figure 3 depicts the envelopes for the oscillation of H, c and ξ over 20 000 time units (equivalent to approximately 700 periods in ξ and 1400 periods in H and c). This picture clearly reveals a decay on the amplitude of oscillation due to the radiation loss. The total decay in amplitude over 20 000 time units is approximately 35%. The total decay may seem to be high. However, careful inspection of the envelopes depicted in Fig. 3 reveals that the decay is approximately equal to 12% for the last half of the run and 5% for the last quarter. This is due to the fact that as the amplitudes of oscillation of H, c and ξ decrease, the soliton resembles the exact stationary solution (which is free of radiation). Therefore, if one wants to obtain steady (or quasi-steady) oscillatory behavior it is necessary to choose configurations with small deviations from the exact solutions.

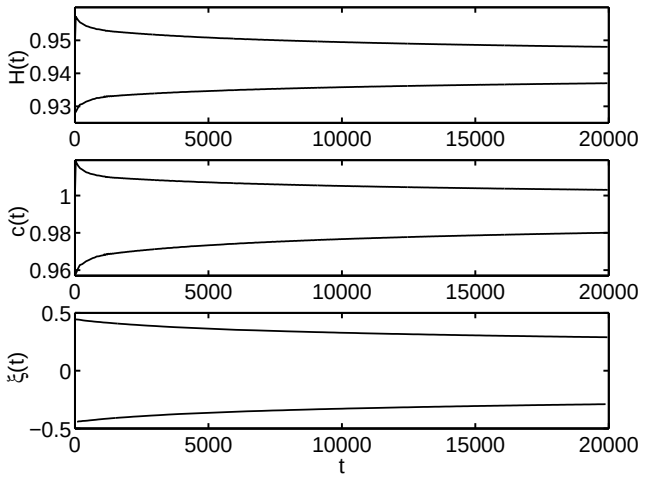

FIG. 3: Damping due to radiation loss. The envelopes for the oscillations in H, c and ξ are depicted over a period $t \in [0, 20\,000]$. The strength of the trapping potential is $V_0 = 0.1$ and the initial soliton's velocity is $v_0 = 0.1$.

III. SOLITON-SOLITON INTERACTION

A. The complex Toda lattice

We now turn our attention to the soliton-soliton interaction for the case of zero potential $V_0 = 0$. This case corresponds to the interaction of solitons in an optical fiber which as received a great deal of attention (see [29–34] and references therein). In this section we give a brief overview of results obtained to reduce the soliton-soliton

interaction to a system of coupled ordinary differential equations (ODEs). The basic idea is based on perturbation techniques using inverse scattering theory [35].

Let us consider the NLS (2) with $V_0 = 0$ and let us suppose we start with an initial condition built from the superposition of single solitons of the form

$$u_j(x,t) = 2\nu_j \mathrm{sech}(z_j(x,t))e^{\mathrm{i}\phi_j(x,t)}, \tag{14}$$

where the index j refers to the jth soliton and with

$$\begin{cases} z_j(x,t) &= 2\nu_j(x-\xi_j(t)), \\ \phi_j(x,t) &= \dfrac{v_j}{\nu_j} z_j(x,t) + \delta_j(t), \\ \xi_j(t) &= 2v_j t + \xi_j(0), \\ \delta_j(t) &= 2(v_j^2+\nu_j^2)t + \delta_j(0). \end{cases} \tag{15}$$

where v_j, ν_j, ξ_j and δ_j are the respective velocities, amplitudes, positions and phases of the jth soliton.

When several solitons are introduced non-trivial interactions occur and their superposition $\sum_j u_j(x,t)$ is no longer a solution of the NLS. Nonetheless, Karpman and Solov'ev obtained an approximation, based upon the inverse scattering transform, for the behavior of two interacting solitons given by a system of ODEs on the soliton parameters [29]. This was later generalized for a train of solitons by Gerdjikov [31, 32]. Their approximation is based upon the ansatz (14) and allowing the 4 parameters for each soliton: v_j, ν_j, ξ_j and δ_j (velocity, amplitude, position and phase) to vary with time. In the particular case that the velocities and amplitudes are small perturbations of a common value, v and ν, and the pulses are well separated,

$$\begin{aligned} |v_j - v| &\ll \nu, \\ |\nu_j - \nu| \ll |\xi_j - \xi_n|^{-1} &\ll \nu, \end{aligned} \tag{16}$$

where $j \neq n$. Within this regime the parameter evolution is follows the system,

$$\begin{aligned} \dot{\nu}_j &= 16\nu^2(\tilde{S}_{j,j-1} - \tilde{S}_{j,j+1}), \\ \dot{v}_j &= -16\nu^2(\tilde{C}_{j,j-1} - \tilde{C}_{j,j+1}), \\ \dot{\xi}_j &= 2v_j \\ \dot{\delta}_j &= 2(v_j^2+\nu_j^2) \end{aligned} \tag{17}$$

where

$$\begin{aligned} \tilde{S}_{j,n} &= e^{-|2\nu(\xi_j-\xi_n)|}\nu \sin s_{jn}\tilde{\phi}_{jn}, \\ \tilde{C}_{j,n} &= e^{-|2\nu(\xi_j-\xi_n)|}\nu \cos \tilde{\phi}_{jn}, \\ \tilde{\phi}_{jn} &= \delta_j - \delta_n - 2v(\xi_j - \xi_n), \\ s_{j,j-1} &= 1 = -s_{j,j+1}. \end{aligned} \tag{18}$$

In fact this system may be reduced to a complex Toda lattice under a simple change of variables [37].

B. The real Toda lattice

We adapt the system above to our lattice problem by making the following additional reductions.

(a) The oscillations are localized and we take the *average* velocity v to be zero.

(b) With $v = 0$, the parameter set for which all amplitudes are equal, $\nu_j = \nu$, and the phase difference between consecutive pulses alternates sign, $\delta_j - \delta_{j\pm1} = \pm\delta$, for all $j \in \mathbb{Z}$ and some δ, is invariant under the flow given by Eqs. (18). We restrict our attention to this set, and take $\delta = \pi$ since this value of an alternating phase shift provides stability, see [34].

With these restrictions, and setting $c \equiv 2\nu$, the equation for the pulse positions uncouples and leads to a real Toda lattice, [37],

$$\ddot{\xi}_j = 8c^3\left(e^{-c(\xi_j - \xi_{j-1})} - e^{-c(\xi_{j+1}-\xi_j)}\right), \tag{19}$$

for all $j \in \mathbb{Z}$.

IV. THE LATTICE DIFFERENTIAL EQUATION

We combine the pulse-potential and pulse train interactions derived in sections II B and III into a model for the dynamics of coupled Bose-Einstein condensates trapped within the periodic potential $V(x)$ as depicted in Fig. 4. In the $k \to 1$ regime of well-spaced potential minima, the periodic potential V can be approximated by a sum of single hump potentials,

$$V(x) = V_0\,\mathrm{sn}^2(x;k) \simeq 1 + \sum_{j\in\mathbb{Z}}\left(\tilde{V}_j(x) - 1\right),$$

where

$$\tilde{V}_j(x) = V_0\,\tanh^2(x - \xi_{0;j}), \tag{20}$$

and the centers of the potentials $\xi_{0;j}$ are given by

$$\xi_{0;j} = 2j\,K(k) = j\Lambda,$$

where $K(k)$ is the complete elliptic integral of the first kind that prescribes the period $\Lambda = 2K(k)$ of the potential.

As an ansatz for our solution, we place a perturbed pulse in each well of the potential,

$$\bar{u}(x) = \sum_{j\in\mathbb{Z}} (-1)^j u(x - \xi_j), \tag{21}$$

where $u(x,t)$ is given as in Eq. (11) and ξ_j lies within $K(k)/2$ of the corresponding minima $\xi_{0;j}$. For the potential (3), when all $\xi_j = \xi_{0;j}$, the ansatz given in Eq. (21)

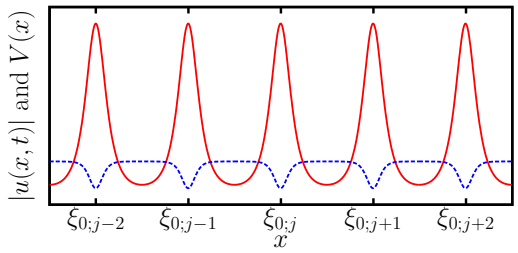

FIG. 4: (Color online) A train of Bose-Einstein condensates (red solid line) at rest on the periodic potential $V(x)$ (blue dashed line).

is an approximation (for k close to 1) to the exact stationary solution

$$u(x) = \sqrt{k^2 - V_0}\,\mathrm{cn}(x;k)\,e^{\mathrm{i}(\frac{1}{2}-k^2+V_0)}, \qquad (22)$$

where $\mathrm{cn}(x;k)$ denotes the Jacobi elliptic cosine. It is important to mention that we are taking a chain of pulses that have alternating signs (i.e., with a relative π phase shift) since the corresponding cn solution (see solid line in Fig. 5) is known to be stable while the chain of equal phase pulse, corresponding to the dn solution (see dashed line in Fig. 5), is unstable [28]. Keeping only the interactions between nearest neighbor pulses and between each pulse and its on-site potential, we have the coupled Lattice differential equation (LDE)

$$\ddot{\xi}_j = 8c^3\left(e^{-c(\xi_j-\xi_{j-1})} - e^{-c(\xi_{j+1}-\xi_j)}\right) - V'_{\mathrm{eff2}}(\xi_j - \xi_{0,j}), \qquad (23)$$

for the pulse positions.

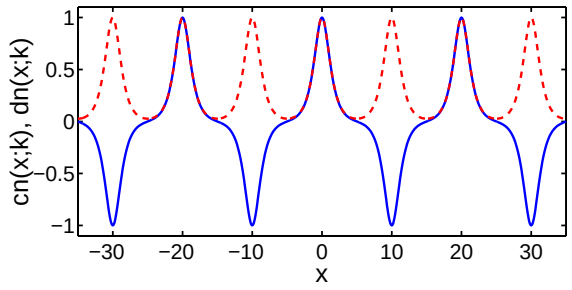

FIG. 5: (Color online) Exact solutions for the GP equation with the periodic potential given in Eq. (3). The blue solid line depicts the $\mathrm{cn}(x;k)$ that corresponds to a stable chain of pulses with alternating phases. The red dashed line depicts the $\mathrm{dn}(x;k)$ solution corresponding to an unstable chain of same phase pulses. The elliptic modulus k is taken near one ($k = 0.999\,636\,205\,4$) such that the spacing between pulses is $\Lambda = 2K(k) = 10$.

We validate the approximations given in the previous section by comparing the dynamics of the full GP equation (2) with the LDE approximations (17) and (23). In Fig. 6 we compare the GP equation dynamics to the LDE (23), both with and without pinning potential, for a system of four pulses in adjacent potentials. Each pulse is given a different initial velocity. The agreement is quantitatively quite good, even over 10 periods of oscillation for the pinned pulses. In Fig. 7 we compare the complex Toda lattice (17) with the LDE (23) without potential. The figure shows a discrepancy of less than 10^{-3} over 500 seconds. These results support the approximations that led to the real Toda lattice, corroborating the reduction of the full GP dynamics (2) to the LDE for the pulse positions when all the pulses are quasi-identical, with large separations and small velocities.

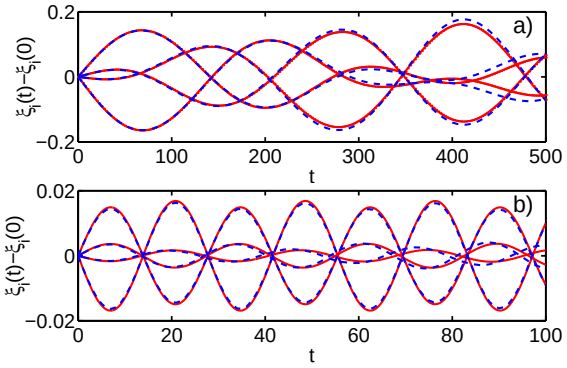

FIG. 6: (Color online) Comparison between the dynamics for interacting solitons in the full PDE (blue dashed lines) and the LDE (23) (red solid lines). The picture depicts the evolution of the relative positions for a chain of 4 identical solitons initially equispaced ($\Lambda = |\xi_{0,j} - \xi_{0,j+1}| = 10$) with small, random, initial velocities. a) Trapless case ($V_0 = 0$) and b) weak trapping case ($V_0 = 0.1$).

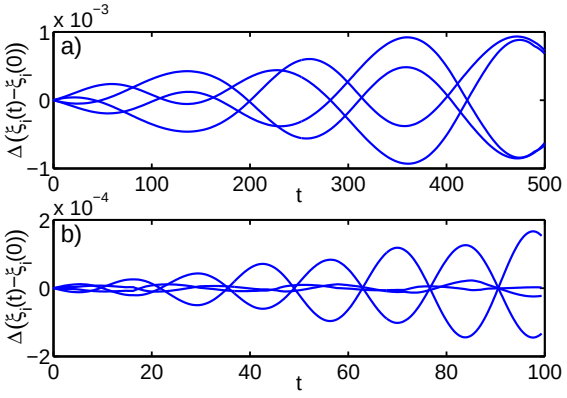

FIG. 7: Comparison between the dynamics for interacting solitons in the complex Toda lattice (17) with the onsite effective potential V_{eff2} (13) and the LDE (23). The panels depict the discrepancy between both models using the same parameters as in Fig. 6.

V. LOCALIZED BREATHERS

We search for spatially localized, oscillatory solutions for GP equation within the LDE reduction (23). We decompose each pulse location into its Fourier modes,

proposing the general ansatz

$$\xi_j(t) = \sum_{k=-\infty}^{+\infty} A_j(k)\, \exp(\mathrm{i}k\omega t), \tag{24}$$

where $A_j(k) = A_j^*(-k)$ (asterisk denoting complex conjugation), and since pulse j is centered at $\xi_{0,j}$ the $k = 0$ coefficient in Eq. (24) satisfies $A_j(0) = \xi_{0,j}$. The general approach of substituting ansatz (24) into the governing lattice equation has been tried in the literature, [38–40], and in principle it is possible to find a relationship for the $A_j(k)$'s. The LDE considered here, Eq. (23), is strongly nonlinear and an exact recurrence relation is difficult to come by. To further reduce the complexity of the model we consider only the first nontrivial mode

$$\xi_j(t) = \xi_{0,j} + A_j\, \cos(\omega t) \tag{25}$$

corresponding to an ansatz where all the solitons oscillate with the same frequency ω and an amplitude to be determined. By substituting Eq. (25) in Eq. (23) one obtains —after Taylor expanding, matching coefficients and keeping first order terms— the following recurrence relation between the oscillating amplitudes of consecutive condensates

$$A_{k+1} = (a + b\, A_k^2)\, A_k - A_{k-1}, \tag{26}$$

with

$$\begin{cases} a &= 2 - \omega^2 + 4\alpha W_0^2 \\ b &= 3\beta W_0^2 \end{cases}$$

where

$$W_0^2 \equiv \frac{1}{16}\frac{e^{c\Lambda}}{c^4},$$

Λ is the periodicity of the potential ($\Lambda = |\xi_{0,j+1} - \xi_{0,j}|$) and α and β are the harmonic and non-harmonic parts of the expansion for the effective potential

$$V'_{\mathrm{eff}}(\xi) = \alpha\xi + \beta\xi^3, \tag{27}$$

as obtained in Eq. (13). It is important to stress that the specific form of the local confining potential is not crucial for the construction of the localized breathes we are interested in. In fact, for the remainder of this section we keep the effective potential as given by its expansion (27). The effective potential coefficients α and β need to be obtained for a specific potential by means of a perturbative approach (as in Sec. II B) or any other suitable technique.

The second order recurrence relation (26) may be cast as a first order system of recurrence equations by defining $y_k = A_k$ and $x_k = A_{k-1}$,

$$\begin{cases} x_{k+1} &= y_k \\ y_{k+1} &= (a + b\, y_k^2)\, y_k - x_k \end{cases} \tag{28}$$

For given α and β we search for frequencies ω for which the two-dimensional (2D) map (28) possesses localized solutions for which (x_k, y_k) decay as $k \to \pm\infty$.

A localized solution for the condensates corresponds to an orbit such that $|A_k| \to 0$ as $k \to \pm\infty$ and such that at least one $|A_j|$ is order one for some j. Such a solution corresponds to a homoclinic orbit connecting the trivial rest state with itself. In terms of the 2D map (28), the desired orbit is a homoclinic connection of the origin $(x, y) = (0, 0)$, which is an fixed point of the 2D map. The trivial orbit, given by $A_k = 0$ for all k, reflects the state with the condensates at rest, i.e., the exact stationary solution (22).

The existence of a homoclinic connection for the origin, requires that the origin be a hyperbolic point, with stable and unstable manifolds. The linearization of the 2D map around the origin yields the following eigenvalues

$$\lambda_\pm = \frac{a \pm \sqrt{a^2 - 4}}{2}. \tag{29}$$

The origin is hyperbolic if one of $\lambda_\pm$ has modulus greater than 1, and one less than 1, which occurs when $|a| > 2$, or equivalently

$$\left|2 + (\Omega^2 - \omega^2)\right| > 2, \tag{30}$$

where

$$\Omega^2 = 4\alpha W_0^2. \tag{31}$$

A typical plot of the stable and unstable manifolds of the origin for the 2D map (28) is depicted in Fig. 8. In Fig. 9 we depict the homoclinic orbit generated by the homoclinic tangle corresponding to the distribution of amplitudes A_k to produce a localized breather in the LDE (23).

VI. CONCLUSIONS

APPENDIX A: CONSERVATION APPROACH

In this appendix we obtain the Newtonian equation of motion that approximates the motion of a single soliton inside a single potential using the conserved quantities of the NLS (2). The conserved quantities of the NLS (2) correspond to total mass and energy:

$$\begin{aligned} N &= \int_{-\infty}^{+\infty} |u|^2\, dx \\ E &= \int_{-\infty}^{+\infty} \left[\frac{1}{2}|u_x|^2 - \frac{1}{2}|u|^4 + |u|^2 V(x)\right] dx. \end{aligned} \tag{A1}$$

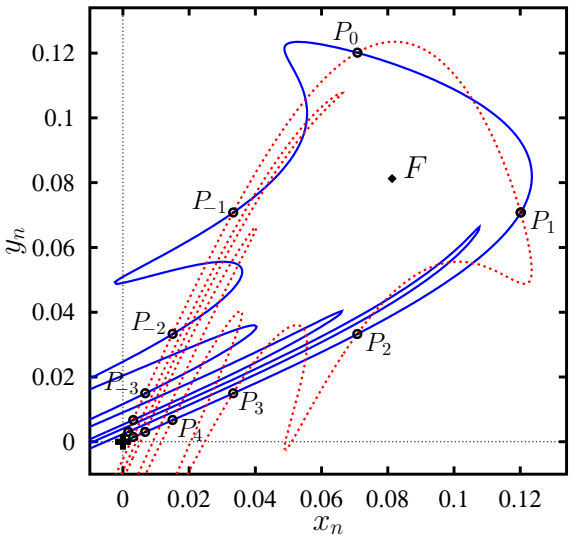

FIG. 8: (Color online) Homoclinic tangle emanating from the origin (hyperbolic) for the 2D map (28). The orbit $\{..., P_{-2}, P_{-1}, P_0, P_1, P_2, ...\}$ belongs to the unstable (red/dashed) and stable (blue/solid) manifolds and thus is mapped forward to $P_{-\infty} = (0, 0)$ and it is mapped backward to $P_{\infty} = (0, 0)$. The parameters used for this figure are: $\Lambda = 10$, $\omega = 17.671$, $V_0 = 0.1$, $c = 1$ for which the 2D map (28) has the coefficients $a = 2.693...$, $b = -104.888...$ and the eigenvalues (29) are $\lambda_- = \lambda_+^{-1} = 0.4448....$

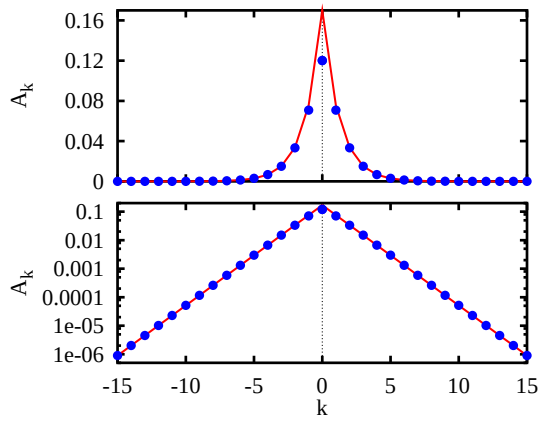

FIG. 9: Homoclinic orbit (blue circles) corresponding to the x-coordinates of the points P_i depicted in Fig. 8. The central amplitude corresponds to $[P_0]_x = 0.1201....$ The bottom panel, displayed in linear-log, clearly depicts the exponential decay rate $\lambda_-^{|k|} = \lambda_+^{-|k|} = (0.4448...)^{|k|}$ (red line) given by Eq. (29).

Inserting the ansatz (6) into Eqs. (A1) and imposing conservation of mass and energy ($dN/dt = 0 = dE/dt$) yields

$$N = \frac{H^2}{\nu} \tag{A2}$$

$$E = \frac{2H^2\nu}{3} + \frac{H^2\dot{\xi}^2}{2\nu} - \frac{H^4}{3\nu} + H^2 V_0 h(2\nu, \xi).$$

where we define the *overlapping integral*

$$h(2\nu, \xi) = \int_{-\infty}^{+\infty} \mathrm{sech}^2(2\nu(x-\xi)) \tanh^2(x)\, dx \tag{A3}$$

Let us now suppose that the variation on the soliton's amplitude and width can be neglected. In fact, as it is shown later, the variations on amplitude and width are very small for small values of V_0. Taking that into consideration and by differentiating the energy with respect to time we obtain

$$\frac{dE}{dt} = \frac{H^2\dot{\xi}\ddot{\xi}}{\nu} + H^2 V_0 \dot{\xi} h_\xi(2\nu, \xi) = 0,$$

and hence,

$$\ddot{\xi} = -V'_{\mathrm{eff1}}(\xi) = -\frac{1}{2} c V_0 h_\xi(c, \xi), \tag{A4}$$

where from now on we also use $c = 2\nu$ as the width of the soliton. Equation (A4) can be considered as the movement of a particle inside a potential well with effective potential $V_{\mathrm{eff1}}(\xi)$. It is important to stress that equation (A4) is an approximation since the ansatz (6) cannot reflect the true dynamics of an oscillating soliton inside a nonlinear potential.

A close form for the effective potential, defined through the integral (A3), cannot be found. Nevertheless, the integral (A3) can be approximated using Taylor expansions around $\nu = 1/2$ ($c = 1$) and $\xi \ll 1$:

$$\begin{aligned} h(c, \xi) &= h(1, \xi) + (c-1) h_c(1, \xi) \\ &\quad + \frac{(c-1)^2}{2} h_{cc}(1, \xi) + O(c^3). \end{aligned} \tag{A5}$$

The above expression involves integrals of the form

$$\int_{-\infty}^{+\infty} x^n \tanh^2(x) \,\mathrm{sech}^{2p}(x-\xi) \tanh^q(x-\xi) dx,$$

for $n = 0, 1, 2$, $p = 1, 2$ and $q = 0, 1$. After evaluating these integrals we obtain the following approximation for the deriavtive of the overlapping integral

$$\begin{aligned} h_\xi(c, \xi) &\approx \frac{8}{15}\left[(1-b)\, c^2 + (-1+2\,b)\, c - b + 2\right] \xi \\ &\quad - \frac{16}{63}\left(19\, c - 8\, c^2 - 9\right) \xi^3 \end{aligned} \tag{A6}$$

where $b = 15\pi^2/63$. As it may be noticed, the effective potential is an even function of ξ reflecting the left-right symmetry of the problem.

Considering again that the variations on amplitude and width of the soliton can be neglected for sufficiently small V_0, the derivative of the effective potential takes the simple form

$$V'_{\mathrm{eff1}}(\xi) \approx c V_0 \left[\frac{8}{15}\xi - \frac{16}{63}\xi^3\right], \tag{A7}$$

which yields the effective potential (8).

APPENDIX B: PERTURBATIVE ANALYSIS

In this appendix we give the details for obtaining a more accurate representation of the effective potential for the bright soliton oscillations inside a single potential well.

Let us start with the perturbed ansatz (11)-(12) and rescale time as $\tau = \sqrt{V_0}\, t$ we now use $\dot{(\cdot)}$ to denote the derivative with respect to the rescaled time τ. Introducing the sliding spatial variable, $y = x - \xi$, inserting the ansatz (11) into the GP equation (2), and equating real and imaginary terms yields,

$$v(t) = \dot{\xi}(t)\sqrt{V_0}, \tag{B1}$$

and, for the real part

$$-V_0(y\ddot{\xi} - \dot{\xi}^2)R - \omega r + \frac{1}{2}(R_{yy} - V_0\dot{\xi}^2 R) = VR. \tag{B2}$$

Taking the potential amplitude, V_0, as a small parameter, we expand the phase, position and shape correction,

$$\begin{aligned}
\omega &= \omega_0 + V_0^2\,\omega_2 + \cdots = \tfrac{1}{2} - V_0 + V_0^2\,\omega_2 + \cdots, \\
\xi &= \xi_0 + V_0\,\xi_1 + \cdots, \\
\psi &= \psi_0 + V_0\,\psi_1 + \cdots,
\end{aligned}$$

and insert Eqs. (12) and (10) into Eq. (B2) to obtain the following equations,

$$\begin{aligned}
O(V_0): &\qquad L\psi_0 = f_1(y), \\
O(V_0^2): &\qquad L\psi_1 = f_2(y),
\end{aligned} \tag{B3}$$

where the first order is zero since we perturbed about an exact solution. The differential operator L is defined by

$$Lv = v_{yy} + (6S^2 - 1)v,$$

and

$$f_1(y) = \left[2\,y\,\ddot{\xi}_0 - \xi_0^2 + 2(\tilde{T}^2 - T^2)\right] S,$$

and

$$\begin{aligned}
f_2(y) &= 6(S^2\psi_0 - \psi_0^2 S) + 2\left(\tilde{T}^2 - 1 + y\,\ddot{\xi}_0 - \tfrac{1}{2}\dot{\xi}_0^2\right)\psi_0 \\
&+ \left(\tfrac{1}{2}\dot{\xi}_0^2 + T^2 - \tilde{T}^2 + 2\,\omega_2 + y(2\ddot{\xi}_1 - \ddot{\xi}_0) - 2\,\dot{\xi}_0\dot{\xi}_1\right) S
\end{aligned} \tag{B4}$$

where, for simplicity, we defined $T = \tanh(y)$ and $\tilde{T} = \tanh(y + \xi)$.

The formal kernel of L is comprised of two linearly independent functions, $H_1(y)$, which decays exponentially at $|y| \to \infty$ and H_2 which grows at infinity. The localized function, H_1, takes the form

$$H_1(y) = S(y)\,T(y),$$

while the unbounded element, H_2, of the kernel of L is found by reduction of order,

$$\begin{aligned}
H_2 &= -H_1 \int \frac{1}{H_1^2} = -S\,T \int \frac{1}{S^2\,T^2} \\
&= -\frac{1}{2}\left(\frac{1}{S} + 3\,y\,S\,T - 3\,S\right).
\end{aligned}$$

The solvability condition for the $O(1)$ equation from Eq. (B3), requires $(f_1, H_1)_2 = 0$, where $(\cdot,\cdot)_2$ denotes the L_2 inner product. However $(yS, H_1)_2 = 1$ while even-odd symmetry implies that $(S, H_1)_2 = (T^2 S, H_1)_2 = 0$, so the solvability condition reduces to,

$$\ddot{\xi}_0 = -(\tilde{T}^2 S, H_1)_2. \tag{B5}$$

At first order in V_0, the this reduces to

$$\ddot{\xi}_0 = -k_0(\xi_0) \tag{B6}$$

where

$$\begin{aligned}
k_0(\xi) &= 8\,\frac{\left((2\xi - 3)\,e^{4\xi} + 8\,\xi\,e^{2\xi} + 2\,\xi + 3\right)e^{2\xi}}{\left(e^{\xi} - 1\right)^4\left(e^{\xi} + 1\right)^4} \\
&\simeq \frac{8}{15}\xi - \frac{16}{63}\xi^3 + \frac{16}{225}\xi^5 + o(\xi^7).
\end{aligned}$$

This ODE corresponds to the motion of a particle inside the effective potential:

$$\begin{aligned}
V_{\text{eff2}}^{(1)}(\xi) &= -\int k_0(\xi)\,d\xi \\
&= -8\,\frac{e^{2\xi}\left(\xi\,e^{2\xi} - e^{2\xi} + 1 + \xi\right)}{\left(e^{2\xi} - 1\right)^3}.
\end{aligned}$$

The full expression for the leading order dynamics, Eq. (B5), can be integrated to yield a closed form relation between $\dot{\xi}$ and ξ. Indeed,

$$\begin{aligned}
\frac{1}{2}\frac{d}{d\tau}\left(\dot{\xi}_0^2\right) &= \dot{\xi}_0\ddot{\xi}_0 = -\dot{\xi}_0 \int T^2(y + \xi_0)\,S^2(y)\,T(y)\,dy \\
&= -\int \dot{\xi}_0\,T^2(y + \xi_0)\,S^2(y)\,T(y)\,dy.
\end{aligned}$$

However,

$$\frac{d}{d\tau}\left(I_T(y + \xi_0)\right) = \dot{\xi}_0\,T^2(y + \xi_0),$$

for $I_T(z) = \int T^2(z)\,dz = z - T(z)$ and therefore,

$$\frac{1}{2}\frac{d}{d\tau}\left(\dot{\xi}_0^2\right) = -\frac{d}{d\tau}\int I_T(y + \xi_0)\,S^2(y)\,T(y)\,dy.$$

Evaluating the integral yields

$$\dot{\xi}_0 = \pm\sqrt{-2\,\Xi(\xi_0) + \frac{2}{3} + \dot{\xi}_0^2(0)}, \tag{B7}$$

where

$$\Xi(\xi) = \int I_T(y+\xi)\, S^2(y)\, T(y)\, dy = \frac{e^{6\xi} - (8\,\xi - 5)\, e^{4\xi} - (8\,\xi + 5)\, e^{2\xi} - 1}{(e^{\xi} - 1)^3\, (e^{\xi} + 1)^3}$$

To compute the perturbations to the pulse shape during the oscillation, and the higher order correction to the pulse motion, we must first solve the $O(V_0)$ equation from Eq. (B3). By variation of parameters we have the general solution

$$\psi_0 = -H_2\, I_1 + H_1\, I_2 + c_1\, H_1 + c_2\, H_2, \qquad \text{(B8)}$$

where

$$I_j = \int \frac{H_j\, f_1}{W(H_2, H_1)},$$

and the Wronskian $W(H_2, H_1) = H_2' H_1 - H_2\, H_1' = 1$. To have $\psi_0 \in L^2(\mathbb{R})$ requires $c_2 = 0$ while to remove degeneracy in the pulse position we impose the condition

$$(\psi_0(y), H_1(y)) = 0, \qquad \text{(B9)}$$

which determines c_1,

$$c_1 = \frac{3}{2}(H_2\, I_1 - H_1\, I_2, H_1). \qquad \text{(B10)}$$

In Fig. 10 we depict a typical shape of the correction to the wave function obtained with the above perturbation analysis.

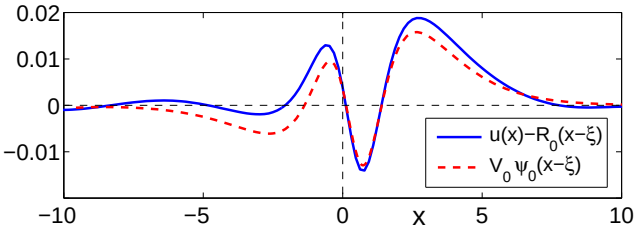

FIG. 10: (Color online). Typical example of the shape correction on the oscillating soliton. The solid line represents the numerical solution to the full NLS (2) minus the unperturbed ansatz $R_0(x-\xi)$ (10). The dynamics for the condensate corresponds to a soliton initially placed at the bottom a potential with strength $V_0 = 0.1$ with an initial velocity of $v_0 = 0.1$. The snapshot for the wave function is taken at the maximum displacement where $\xi(t) \simeq 0.42$. The dashed line represents the first order correction to the shape: $V_0\, \psi_0(x-\xi, V_0)$ given by Eq. (B8).

The next order correction to the pulse dynamics follows from the solvability condition for the $O(V_0^2)$ equation in Eq. (B3), which may be written as

$$\ddot{\xi}_1 = -k_1(\xi_0), \qquad \text{(B11)}$$

where using Eqs. (B5) and (B9) yields

$$k_1(\xi_0) = (\tilde{T}^2\psi_0, H_1) + \ddot{\xi}_0(y\psi_0, H_1) - 3(\psi_0^2 S - \psi_0 S^2, H_1). \qquad \text{(B12)}$$

In the limit of small amplitude oscillations this takes the form

$$k_1(\xi_0) = -\frac{224}{1125}\xi_0 + \left(\frac{1}{36}\pi^2 + \frac{7}{18}\right)\ddot{\xi}_0\, \xi_0^2 + O(\xi_0^3). \qquad \text{(B13)}$$

Combining Eqs. (B6) and (B11) yields an explicit equation for the oscillatory motion of the condensate within the potential $V(x)$,

$$\ddot{\xi} = -V_{\text{eff2}}'(\xi) = -V_0\, k_0(\xi) - V_0^2\, k_1(\xi) + O(V_0^3),$$

which has the following explicit form in the small amplitude limit,

$$V_{\text{eff2}}'(\xi) = V_0\left[\left(\frac{8}{15} - \frac{224}{1125}V_0\right)\xi - \frac{16}{63}\xi^3\right] + O\left(V_0^3\xi, \xi^4\right).$$

yielding the effective potential (13).

[1] S.N. Bose. *Z. Phys.*, **26** (1924) 178–181.
[2] A. Einstein. *Sitz. Preuss Akad. Wiss.*, **1924** (1924) 261–267.
[3] M.H. Anderson, J.R. Ensher, M.R. Matthews, C.E. Wieman and E.A. Cornell. *Science*, **269** (1995) 198–201.
[4] K.B. Davis, M.-O. Mewes, M.R. Andrews, N.J. van Drutten, D.S. Durfee, D.M. Kurn and W. Ketterle. *Phys. Rev. Lett.*, **75**, 22 (1995) 3969–3973.
[5] P.G. Kevrekidis, D.J. Frantzeskakis, and R. Carretero-González (eds). *Emergent Nonlinear Phenomena in Bose-Einstein Condensates: Theory and Experiment*. Springer Series on Atomic, Optical, and Plasma Physics, Vol. **45**, 2008.
[6] E.P. Gross. *Nuovo Cim.*, **20** (1961) 454–461.
[7] L.P. Pitaevskii. *Sov. Phys. JETP*, **13** (1961) 451–454.
[8] F. Dalfovo, S. Giorgini, L.P. Pitaevskii and S. Stringari. *Rev. Mod. Phys.*, **71**, 3 (1999) 463–512.
[9] F.S. Cataliotti, S. Burger, C. Fort, P. Maddaloni, F. Minardi, A. Trombettoni, A. Smerzi and M. Inguscio. *Science*, **293** (2001) 843–846.
[10] M. Greiner, I. Block, O. Mandel, T.W. Hänsch and T. Esslinger. *Appl. Phy. B*, **73**, 8 (2001) 769–772.
[11] A. Trombettoni and A. Smerzi. *Phys. Rev. Lett.*, **86**, 11 (2001) 2353–2356.
[12] F.Kh. Abdullaev, B.B. Baizakov, S.A. Darmanyan, V.V. Konotop and M. Salerno. *Phys. Rev. A*, **64**, 4-6 (2001) 043606.
[13] A. Smerzi, A. Trombettoni, P.G. Kevrekidis and A.R. Bishop. *Phys. Rev. Lett.*, **89** (2002) 170402.
[14] F.S. Cataliotti, L. Fallani, F. Ferlaino, C. Fort, P.

Maddaloni, M. Inguscio, A. Smerzi, A. Trombettoni, P.G. Kevrekidis and A.R. Bishop. Preprint: cond-mat/0207139 (2002).
[15] M. Key, I.G. Hughes, W. Rooijakkers, B.E. Sauer, E.A. Hinds, D.J. Richardson and P.G. Kazansky. *Phys. Rev. Lett.*, **84**, 7 (2000) 1371–1373.
[16] N.H. Dekker, C.S. Lee, V. Lorent, J.H. Thywissen, S.P. Smith, M. Drndć, R.M. Westervelt and M. Prentiss. *Phys. Rev. Lett.*, **84**, 6 (2000) 1124–1127.
[17] J. Reichel, W. Hädnsel and T.W. Hänsch. *Phys. Rev. Lett.*, **83** (1999) 3398.
[18] J. Reichel, W. Hänsel, P. Hommelhoff and T.W. Hänsch. *Appl. Phy. B*, **72** (2000) 81.
[19] W. Hänsel, J. Reichel, P. Hommelhoff and T.W. Hänsch. *Phys. Rev. Lett.*, **86**, 608 (2001).
[20] A.D. Jackson, G.M. Kavoulakis and C.J. Pethick. *Phys. Rev. A*, **58**, 3 (1998) 2417–2422.
[21] V. Pérez-García, H. Michinel and H. Herrero. *Phys. Rev. A*, **57**, 5 (1998) 3837–3842.
[22] P.A. Ruprecht, M.J. Holland and K. Burnett. *Phys. Rev. A*, **51** (1995) 4704–4711.
[23] R. Carretero-González and K. Promislow, Phys. Rev. A, **66** 033610 (2002).
[24] L. Salasnich, A. Parola and L. Reatto. *Phys. Rev. A*, **66** (2002) 043603.
[25] L. Salasnich, A. Parola and L. Reatto. *Phys. Rev. A*, **65** (2002) 043614.
[26] Y.B. Band, I. Towers and B.A. Malomed. *Phys. Rev. A*, **67** (2003) 023602.
[27] R. Scharf and A.R. Bishop. *Phys. Rev. E*, **47**, 2 (1993) 1375–1383.
[28] J.C. Bronski, L.D. Carr, R. Carretero-González, B. Deconinck, J.N. Kutz and K. Promislow. *Phys. Rev. E*, **64** (2001) 056615.
[29] V.I. Karpman and V.V. Solov'ev. *Physica D*, **3**, 1/2 (1981) 142–164.
[30] V.I. Karpman and V.V. Solov'ev. *Physica D*, **3** (1981) 487–502.
[31] V.S. Gerdjikov, D.J. Kaup, I.M. Uzunov and E.G. Estaviev. *Phys. Rev. Lett.*, **77**, 19 (1996) 3943–3946.
[32] V.S. Gerdjikov, I.M. Uzunov, E.G. Estaviev and G.L. Diankov. *Phys. Rev. E*, **55**, 5 (1997) 6039–6060.
[33] J.M. Arnold. *J. Opt. Soc. Am. A*, **15**, 5 (1998) 1450–1458.
[34] J.M. Arnold. *Phys. Rev. E*, **60**, 1 (1999) 979–986.
[35] V.V. Konotop and L. Vázquez. *Nonlinear random waves*. World Scientific Publishing, 1994.
[36] A. Scott. Oxford Univ. Press, 1999.
[37] Morikazu Toda. *Theory of Nonlinear Lattices*. Springer-Verlag, second enlarged edition edition, 1989.
[38] Y.S. Kivshar. *Phys. Rev. E*, **48**, 1 (1993) R43–R45.
[39] S. Flach and C.R. Willis. *Phys. Rep.*, **295** (1998) 181–264.
[40] T. Bountis, H.W. Capel, M. Kollmann, J.C. Ross, J.M. Bergamin and J.P. van der Weele. *Phys. Lett. A*, **268**, 1/2 (2000) 50–60.
[41] J.C. Bronski, L.D. Carr, B. Deconinck and J.N. Kutz. *Phys. Rev. E*, **63** (2001) 036612.
[42] J.C. Bronski, L.D. Carr, B. Deconinck and J.N. Kutz. *Phys. Rev. Lett.*, **86**, 8 (2001) 1402–1405.
[43] V. Pérez-García, H. Michinel, J.I. Cirac, M. Lewenstein and P. Zoller. *Phys. Rev. A*, **56**, 2 (1997) 1424–1432.
[44] V. Pérez-García, H. Michinel, J.I. Cirac, M. Lewenstein and P. Zoller. *Phys. Rev. Lett.*, **77**, 27 (1996) 5320–5323.